Proceedings of the 28th IEEE
EMBS Annual International Conference
New York City, USA, Aug 30-Sept 3, 2006

Automatic Microtubule Tracking for QD-Based In Vivo Cell Imaging and Drug Efficacy Study

Koon Yin Kong, Adam I. Marcus, Jin Young Hong, Paraskevi Giannakakou, and May D. Wang

Abstract— **Microtubules (MT) are dynamic polymers that rapidly transition between states of growth, shortening, and pause. These dynamic events are critical for many microtubule functions such as intracellular trafficking and signaling. In addition, cancer chemotherapy drugs that target microtubules, such as the taxanes and the vinca alkaloids, are known to suppress microtubule dynamics at low doses, leading to mitotic arrest and cell death. Quantification of microtubule dynamics can be used as a read-out of anticancer-drug activity and can be a surrogate marker of drug sensitivity/resistance. The emerging nanotechnology such as quantum dots has provided properties such as less photo bleaching, higher probe imaging intensity, better specificity and sensitivity, which finally makes visualizing subcellular events over long enough time a possibility. But it also results in big increase in data acquisition. The traditional way of annotating MT manually is becoming a daunting task. Thus, the goal is to research and develop an efficient, reliable, and rapid MT tracking. In this paper, we describe active contour-based [1] tracking methods to automatically track MT. We redefine the internal energy terms specifically for open snake, and examine different external energy terms for locating the end tips of a microtubule. This algorithm has been validated using simulated images, images of untreated MCF-7 breast cancer cells, and image of cells treated with the microtubule-targeting chemotherapeutic agent, Taxol**

I. Introduction

The advent of new fluorescent microscopy technologies have allowed for the rapid acquisition of dynamic cellular processes with both high spatial and temporal resolution. In addition, the new bioconjugate Quantum Dots (QD) imaging probes provide much higher imaging intensity, specificity, sensitivity with much less photo bleaching in comparing to traditional fluorescence dyes. As a result, the cell activities can be acquired over a long time with huge amounts of data. However, the automatic data processing falls behind and the analyses are typically performed manually. This daunting task can be cumbersome, time-consuming and often lead to human error. Thus, there is an urgent need for data analysis system that can automatically track MT dynamics to bridge the gap between data acquisition and data analysis.

Microtubule dynamics refers to the stochastic nature of microtubule movement, where microtubules transition between events of slow growth, rapid shortening, and pause [2]. These movements are due to the addition or removal of alpha and beta tubulin dimers, the primary constituent of the microtubule polymer. In cells, this process is controlled by GTP-hydrolysis and is tightly-regulated by microtubule-associated proteins [3]. Microtubule dynamicity plays critical role in cell division; in particular, microtubules must reorganize from interphase to form a bipolar microtubule spindle that aligns and segregates chromosomes equally into the daughter cells. To do this properly, microtubule dynamicity increases about 10 to 100 fold as the cell transitions into mitosis [4]. Due to this vital role in cell division, microtubules have become excellent anti-cancer targets, and are the primary target for perhaps the most successful cancer chemotherapeutic, paclitaxel.

Paclitaxel is a member of a class of microtubule-targeting agents known as the taxanes, which bind directly to the microtubule polymer. Upon taxol binding, microtubule dynamics are suppressed and microtubule morphology changes, such that individual microtubules associate with one another, forming microtubule bundles. The end result is microtubule stabilization, which leads to mitotic arrest and eventual cell death [5]. Notably, it appears that suppression of microtubule dynamics is the critical factor for taxol-induced cell death, since low doses of the drug that suppress microtubule dynamics, but do not result in microtubule bundles, are enough to trigger mitotic arrest and subsequent cell death [6]. Furthermore, it has been shown that cellular resistance to taxol, which hampers the clinical efficacy of the drug, may be due to enhanced microtubule dynamics; Goncalves et al. [7] have shown that microtubule dynamics is significantly increased in taxol-resistant lung cancer cells, suggesting that cells may overcome taxol-induced dynamic suppression by maintaining a higher state of dynamic instability. Thus it is clear, that a better understanding of

Manuscript received July 10, 2006. This research has been supported by grants from National Institutes of Health (Bioengineering Research Partnership R01CA108468, P20GM072069, Center of Cancer Nanotechnology Excellence U54CA119338), and Georgia Cancer Coalition (Distinguished Cancer Scholar Award to Professor Wang).; and by NIH grants R01CA100202, R01CA114335 awarded to Paraskevi Giannakakou and 1PO1CA116676-01A1 to Paraskevi Giannakakou and Adam Marcus.

Koon Yin Kong is with the School of Electrical and Computer Engineering, Georgia Institute of Technology, Atlanta, GA 30332, USA (E-mail: kykong@gatech.edu).

Adam I. Marcus is with the Winship Cancer Institue, Emory University, Atlanta, GA 30322, USA (E-mail: Adam.Marcus@emoryhealthcare.org).

Jin Young Hong is with the Wallace H. Coulter Department of Biomedical Engineering, Georgia Institute of Technology and Emory University, Atlanta, GA, USA

Paraskevi Giannakakou is with the Weill Cornell medical College of Cornell University, New York, NY 10021, USA (E-mail: pag2015@med.cornell.edu)

May D. Wang is with the School of Electrical and Computer Enginerring, the Wallace H. Coulter Department of Biomedical Engineering, and the Winship Cancer Institute, Georgia Institute of Technology and Emory University, Atlanta, GA 30322, USA (E-mail: maywang@bme.gatech.edu).

microtubule dynamics will be beneficial for understanding the mechanisms of, and resistance to, microtubule-targeting agents.

To automatically track MT dynamics, we conduct image enhancement, segmentation, and tracking. We use matched filter of different orientations to improve the contrast of the original images. Then we apply an open-ended snake to do the segmentation and tracking.

II. IMAGE ENHANCEMENT

In this section, we discuss the image processing techniques that are used to detect tube-like structures. Since microscopy and angiography images both have bright curvilinear structure on dark background, many of the processing techniques have their origins from applications in angiography images. We first examined segmentation of curvilinear structure, such as retinal blood vessel [8][9]. Chutatape [8] uses Gaussian matched filter to enhance retinal blood vessels from the background, and segments by an extended Kalman filter to predict and update the location of the next vessel pixel using the information from the previously segmented pixels. Hoover describes another retinal vessel segmentation algorithm [9], which uses matched filter to enhance the original image, and segments using local threshold and morphological filters to test local and region-based properties.

A typical frame of a microtubule image consists of bright and dark pixels which correspond to microtubule and background pixels respectively. Using intensity threshold alone is not enough to detect microtubules from the background because the intensity distribution is not bimodal. Many noise pixels have mid-range intensity, falling between the microtubule and background intensities. To remove those noises and enhance the image, we use matched filters.

Matched filtering is a technique used to increase the contrast, or the signal to noise ratio. We use an inverted second derivative of a Gaussian function in a rectangular mask to approximate the shape of a microtubule segment. Mask pixels that are located along the center line of the rectangle have the highest values and the values decay exponentially away from the center line throughout the mask area. Normalization is used so that the response of a constant intensity area is zero. One drawback of using matched filter is that it could amplify noise that is in the background region. We select Otsu's automatic thresholding method [10] to limit this artifact.

III. OPEN ENDED SNAKE

After every frame is enhanced using matched filter and thresholding, we proceed to track the position of each microtubule along time. Since microtubules are line structures, we use snake to do the segmentation. First, we use the snake to align to nearby edges that correspond to microtubules structure. Next we shrink the snake to account for shortening of microtubules, and we stretch the snake to account for lengthening. Last we define and compare parameters that govern the snake during the shrinking and growing phase of the microtubule. Because microtubules are very narrow; traditional closed-contour snake cannot accurately track this thin line structure. We propose an open-ended snake to solve this problem. The open ended snake first aligns to nearby microtubules, and then it shrinks and expands to fit the contour to a microtubule.

Similar to traditional snake, an open-ended snake will be guided to desired features defined by the external forces. In our design, the desired features are microtubule structures and microtubule tips. Microtubule structures are represented by matched filter output and gradient vector field of the matched filter output, while microtubule tips are represented by "tip-ness" measure defined using gradient information. How an open-ended snake is different from a normal snake is the formulation of its internal energy. Instead of wrapping the first and the last snaxel to form closed contour, we define two new internal energy terms to make open snake possible. Both of the terms are applied only to the two end points of a snake so that an original closed contour becomes an open one.

To make the snake attract to line feature, we use the output of the matched filter as the external image energy force. Thus the snake energy becomes

$$E_{snake} = \int_0^1 E_{\text{int}}(v(s)) + I_{matchedfil\ ter}(v(s))ds \quad (1)$$

To further assist the snake to move to line feature, we add gradient vector field [11] (GVF) to the internal energy. We define the external constraint such that each snaxel converge to the center of nearby line features by moving in the direction of gradient vector field. The constraint is defined as

$$|\overrightarrow{dv}(s) - \vec{I}_{GVF}(s)| \quad (2)$$

For each possible new snaxel location, the above energy term is minimized. If a snaxel is near an edge, this energy will move the snaxel toward to center of the edge. After it reaches the center of an edge, gradient vector field is small, making the snaxel stay near the center line structures.

Next we want the snake to converge to tip points of a microtubule. To do that, we define a "tip-ness" measure that is based on corner detectors as image feature for the snake. First one is a Haralick detector [12] which uses gradient information to detect corner/end-points. For an image f(x,y) and a local neighborhood c, we form a normal matrix using its partial derivatives

$$N = \begin{bmatrix} \sum_c f_{xx}(x,y) & \sum_c f_{xy}(x,y) \\ \sum_c f_{yx}(x,y) & \sum_c f_{yy}(x,y) \end{bmatrix} \quad (3)$$

Haralick defines the corner measure as the determinant of the normal matrix.

$$w(r,c) = \det(N) \quad (4)$$

Another one is a Plessey [13] corner detector. It uses the structure tensor to detect corners. The structure tensor is

$$N = \begin{bmatrix} \sum_c f_x^2(x,y) & \sum_c f_x(x,y)\cdot f_y(x,y) \\ \sum_c f_x(x,y)\cdot f_y(x,y) & \sum_c f_y^2(x,y) \end{bmatrix} \quad (5)$$

And the cornerness measure is

$$q(x,y) = \frac{\det(N)}{trace(N)} = \frac{\sum_c f_x^2(x,y)\cdot\sum_c f_y^2(x,y) - \left(\sum_c f_x(x,y)\cdot f_y(x,y)\right)^2}{\sum_c f_x^2(x,y) + \sum_c f_y^2(x,y)} \quad (6)$$

We break down the segmentation process into three steps to account for alignment, shortening, and lengthening. During the alignment process, we use the matched filtered image and the GVF as image energy. After that, using a "tip-ness" measure, a snake which favors shrinking is used to track any shortening of microtubule. To account for lengthening, we replace the snake with an internal energy that favors extension of the snake.

For a closed contour, all derivatives are calculated using neighboring contour points, or snaxels. With open contour, we need to address the boundary condition. We can replace the calculation of derivatives with only snaxel from one side of the snake instead of with both sides. However, in the absence of external force, minimizing this first derivative is similar to minimizing the distance between snaxels. The result is that the snake will shrink into a point. To avoid the shrinking of snake when using first derivative as the internal energy, we replace the internal energy of the two end points with the point distance from the line form by the nearest two snaxels. Fig 1.a) shows the geometry of the distance.

We use the point distance measure to approximate the smoothness term at the end points. The end point of the snake will move only to align with the last two snaxels, thus the shrinking under constant external force is avoided. The distance d(x,y) is defined as

$$d = \frac{|(s_x^{n-2} - s_x^{n-1})(s_y^{n-1} - s_y^n) - (s_x^{n-1} - s_x^n)(s_y^{n-2} - s_y^{n-1})|}{\sqrt{(s_x^{n-2} - s_x^{n-1})^2 + (s_y^{n-2} - s_y^{n-1})^2}} \quad (7)$$

Internal energy of other snaxels in the middle of the contour remains unchanged. We use the matched filter response as the image energy for the snake, along with the proposed modification of internal energy that uses (7). Gradient vector field is also used to extend the capture range of the snake.

To allow the end points to shrink, we stop using the point line distance formulation. Instead, we use the first difference measure between the end point and the snaxel that is closest to it as the internal force. This will shrink the snake, but using the tip-ness measure as image energy could counteract the internal force.

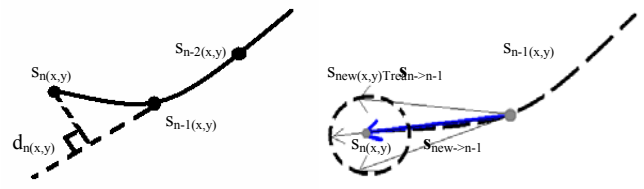

a) Internal energy during shrinking b)

Fig. 1. Modified Internal Energy and Extension Force at the End Points.

To account for lengthening of microtubule, we modify the internal force to favor extension. We extend end point along the direction of the two closest snaxels. Similar to a balloon force which extend snaxel along the normal of the contour, the extension force extend snaxel along the contour itself. For an end point s_n and its closest neighbor s_{n-1}, we try to find a new point s_{new}, such that the dot product, d, from s_{new} to s_{n-1}, and from sn to s_{n-1} is maximized

$$d = \mathbf{s}_{new->n-1} \cdot \mathbf{s}_{n->n-1} \quad (8)$$

Maximizing this quantity will result in new snaxel that is located furthest away from sn-1 along the direction formed by s_n to s_{n-1}. Since extending the snaxel could cause convergence problem, we only extend the snake after the shrinking step, so the snake will only extend along a known edge, thus stability is ensured. Fig. 1b) illustrates the extension force. Dash line shows one end of the open snake, with the end point $s_n(x,y)$ and its closest neighbor $s_{n-1}(x,y)$. The thick blue arrow is $\mathbf{s}_{new->n-1}$, and the thin black arrow is $\mathbf{s}_{n->n-1}$. Dotted circle indicates the search neighborhood where new extended point is found.

IV. RESULTS

We have applied the algorithm to time-lapsed images captured with confocal microscopy. The resolution of the video is 1344x1024 pixels and each microtubule has a width of ~1-2 pixels. Forty one frames are processed, with the first frame as the initial frame. Testing on real microtubule image is shown in Fig. 2. We show the tracked microtubule at from frame number 1, 5, 10, and 20 of 41-frame sequence.

We compare the result of manual quantification (solid line) and open snake (dotted line) using both control MCF7 cell line and PTX treated cell line. Fig 2. and 3 show the results.

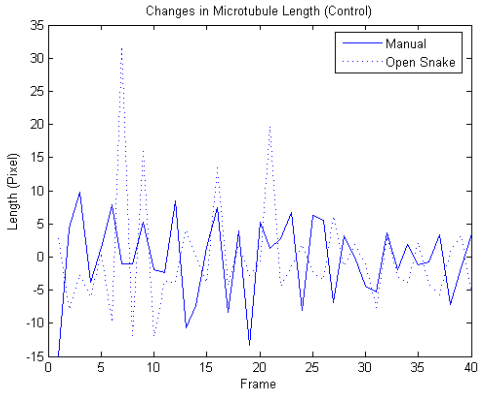

Fig. 2. Comparison of Manual and Open Snake Tracking Results (Control).

In the control, microtubule length changes with larger magnitude than that of the PTX treated microtubule. The difference between manual and open snake is due to the different measure microtubule length measure method. Manual quantification only finds the change of distance from the plus end to a fixed point in the first frame. Open snake calculate the length along the microtubule in each frame.

We also calculate some of the statistics in both image sequences. They are summarized in Table I and II. Result from open snake algorithm agrees with manual quantification

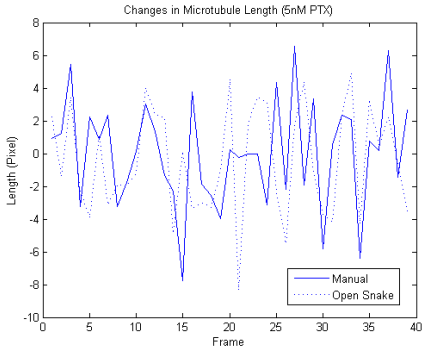

Fig. 3. Comparison of Manual and Open Snake Tracking Results (PTX treated).

result. Once the cell is treated with PTX, the dynamicity is lowered when measured in both ways. Microtubule spends more time in the pause stage and less time in growing and shortening stages.

V. Methodology for Cell Culture and Manual Tracking Microtubules

Manual tracking of microtubules and cell culture was performed essentially as described in Marcus et al. (Cancer Research 2005). In brief, MCF-7 breast cancer cell lines stably expressing a GFP-α-tubulin microtubule reporter protein (kind gift of Dr. Mary Ann Jordan) were used for imaging. Cells were plated on live cell imaging chambers (Mattek) in RPMI 1640 media with 10% fetal bovine serum. Cells were allowed to adhere overnight in a temperature and humidity controlled incubated set at 37°C with 5% CO2. Images were acquired using a Perkin Elmer Ultraview ERS spinning disc confocal mounted on a Zeiss Axiovert (Thornwood, NJ) microscope. A 100X Apochromat (N.A.=1.4) oil lens was used to visualize cells and multiple optical sections (z-distance between sections = 0.5 µm) were captured every three seconds using a Hamamatsu Orca ER camera (Middlesex, NJ) for two minutes (250-400 s exposure. A heating chamber that encapsulated the microscope was used to maintain the temperature at 37 ±0.5°C along with 5% CO2 perfusion. Microtubules ends at the lamellar edge of interphase cells were imaged and subsequently tracked using the "track points" feature on Metamorph image analysis software (Universal Imaging, Downingtown, PA). The coordinates generated from this tracking feature were used to determine the distance individual microtubule ends changed from a fixed point. These values were transferred to a Microsoft Excel spreadsheet and used to generate life history plots of individual microtubules. From these graphs, the various parameters of microtubule dynamicity were calculated.

VI. Discussion

Overall, our proposed method can conduct automated microtubule analysis repeatedly with consistent quality. Also, it can reduce the time it takes to measure microtubule

TABLE I
Microtubule Statistics (Control)

	Manual	Open Snake
Pause	50%	57.5%
Shorten	25%	27.5%
Lengthen	25%	15%
Dynamicity (pixel/frame)	3.8371	4.2525

TABLE II
Microtubule Statistics (Treated with 5nM PTX)

	Manual	Open Snake
Pause	84.62%	61.54%
Shorten	7.69%	20.51%
Lengthen	7.69%	17.95%
Dynamicity (pixel/frame)	0.9332	2.7762

dynamics. The field testing has shown that with same quality, this computer assisted microtubule dynamics systems has been preferred over manual analysis due to its speed and reproducibility. Further research is to track some large movements of microtubules that are not possible to accurately track using open snake alone. This MT tracking system, in combination with Quantum Dot imaging, will make the modeling of MT dynamics in live cell imaging a possibility.

References

[1] M. Kass, A. Witkin, D. Terzopolous, "Snakes: Active Contour Models", International Journal of Computer Vision, 1(4), 1987, 321-331.
[2] Heald, R., and Nogales, E. (2002) J Cell Sci 115, 3-4
[3] H. Maiato, P. Sampaio, and C. E. Sunkel, (2004) Int Rev Cytol 241, 53-153.
[4] Wilson, L., Panda, D., and Jordan, M. A. (1999) Cell Struct Funct 24, 329-335
[5] Jordan, M. A., and Wilson, L. (2004) Nat Rev Cancer 4, 253-265
[6] Jordan, M. A., Toso, R. J., Thrower, D., and Wilson, L. (1993) Proc Natl Acad Sci U S A 90, 9552-9556
[7] Goncalves, A., Braguer, D., Kamath, K., Martello, L., Briand, C., Horwitz, S., Wilson, L., and Jordan, M. A. (2001) Proc Natl Acad Sci U S A 98, 11737-11742
[8] A. Hoover, V. Kouznetsova, M. Goldbaum , "Locating blood vessels in retinal images by piecewise threshold probing of a matched filter response.", IEEE Transactions on Medical Imaging, Mar 2000, 19(3):203-10.
[9] O. Chutatape, L. Zheng, S. Krishman, "Retinal Blood VesselDetection and Tracking by Matched Gaussian and Kalman Filters", Proceeding of IEEE International Previous Frame Current Frame Microtubule Structure Previous Point Search Window IEEE Engineering in Medicine and Biology Society, Vol. 20, No 6, 1998.
[10] N. Otsu, "A Threshold Selection Method from Gray-Level Histograms", IEEE Trans Sys Man Cyberb 9(1): 62-66, 1979.
[11] C. Xu and J. L. Prince, "Gradient Vector Flow: A New External Force for Snakes", Proc. IEEE Conf. on Comp. Vis. Patt. Recog. (CVPR), Los Alamitos: Comp. Soc., pp. 66-71, June 1997.
[12] P.R. Beaudet: *"Rotationally Invariant Image Operators"*, Proc. Intl. Joint Conf. on Pattern Recognition, Kyoto, Japan, 1978, pp. 579-583.
[13] W. Förstner: *"A feature based correspondence algorithms for image matching"*, Intl. Arch. Photogrammetry and Remote Sensing, vol. 24, pp 160-166, 1986.
[14] X. C. He, N. H. C. Yung, "Curvature Scale Space Corner Detector with Adaptive Threshold and Dynamic Region of Support", 17th International Conference on Pattern Recognition, vol. 2, pp. 791-793, 2004.